ORIGINAL RESEARCH

DOI: 10.14744/globecc.2026.22535
Glob Emerg Crit Care 2026;5(4):234-242

Macroscopic Surrogates of Tumor Heterogeneity: Spatial Distribution of Non-Mass Enhancement Predicting Ki-67 Proliferation

Mahmut Küsbeci[1], Umut Deniz Pak[1], Özlem Sezgin Okçu[2], Ayşenur Oktay Alfatlı[2], Işıl Bilgen[2]

[1]*Division of Interventional Radiology, Department of Radiology, Ege University Faculty of Medicine, İzmir, Türkiye*
[2]*Department of Radiology, Ege University Faculty of Medicine, İzmir, Türkiye*

Abstract

Objective: Managing non-mass enhancement (NME) on breast MRI is challenging due to its histological and molecular heterogeneity. This study evaluated the correlation between BI-RADS NME descriptors and histopathological diagnoses, specifically investigating the predictive value of NME distribution patterns regarding breast cancer molecular subtypes and the Ki-67 proliferation index.

Materials and Methods: We retrospectively evaluated 61 patients (62 isolated NME lesions) who underwent dynamic contrast-enhanced breast MRI. Lesions were characterized by distribution patterns, internal enhancement, kinetic curves, and background parenchymal enhancement (BPE). Malignant lesions were analyzed for immunohistochemical profiles (ER, PR, HER2) and the Ki-67 index to determine molecular subtypes.

Results: Of the 62 lesions, 41 (66.1%) were malignant and 21 (33.9%) were benign. Spatial distribution strongly predicted malignancy (p=0.002); focal distribution was predominantly benign, whereas segmental and diffuse patterns indicated malignancy. NME distribution strongly correlated with cellular proliferation: 100% of malignant lesions with focal distribution exhibited a low Ki-67 index (<10%). Marked BPE and asymmetric enhancement were also significantly correlated with malignancy (p=0.020).

Conclusion: NME distribution patterns serve as macroscopic imaging surrogates for tumor heterogeneity. The correlation between focal NME and a low Ki-67 index highlights MRI's potential to noninvasively assess tumor biological aggressiveness. Integrating these features into clinical practice may offer a useful risk stratification tool, laying a preliminary foundation for future radiogenomic predictive models.

Keywords: BI-RADS, breast MRI, Ki-67 index, non-mass enhancement, tumor heterogeneity

Introduction

Breast cancer remains the most prevalent malignancy among women globally, with patient survival closely associated with tumor size and lymph node involvement at the time of diagnosis [1]. Although the incidence of breast cancer continues to rise, associated mortality has declined significantly in recent years, largely due to advances in treatment and the widespread adoption of screening mammography, which has been shown to reduce mortality by up to 30–40% [1,2]. However, mammography has inherent limitations; it fails to detect approximately 9–16% of breast cancers, and its diagnostic sensitivity is markedly reduced in patients with dense breast parenchyma [3–5].

To overcome these limitations, magnetic resonance imaging (MRI) has emerged as a crucial diagnostic and problem-solving tool in breast imaging [4,6–8]. Dynamic contrast-enhanced MRI (DCE-MRI) significantly improves the sensitivity of breast cancer detection by enabling quantitative and qualitative evaluation of contrast enhancement kinetics, which indirectly reflect tumor-induced angiogenesis and capillary permeability [9].

Despite advances in imaging, breast cancer remains a biologically heterogeneous disease [10]. Traditional anatomical staging systems (TNM) are often insufficient to fully predict tumor behavior and patient outcomes [10,11]. Consequently, clinical decision-making now relies heavily on tumor biology and specific prognostic markers, including histological grade, lymph node status, and the

Address for Correspondence: Mahmut Küsbeci, Division of Interventional Radiology, Department of Radiology, Ege University Faculty of Medicine, İzmir, Türkiye
E-mail: drmahmutkusbeci@gmail.com **ORCID-ID:** 0000-0002-7583-1170

Received: 03.09.2026 **Revised Date:** 19.10.2026 **Accepted:** 15.11.2026

Cite this article as: Küsbeci M, Pak UD, Sezgin Okçu Ö, Oktay Alfatlı A, Bilgen I. Macroscopic Surrogates of Tumor Heterogeneity: Spatial Distribution of Non-Mass Enhancement Predicting Ki-67 Proliferation. Glob Emerg Crit Care 2026;5(4):234-242.

Copyright@Author(s) - Available online at https://globemcc.com/
Content of this journal is licensed under a Creative Commons Attribution-NonCommercial 4.0 International Licens

expression of estrogen receptor (ER), progesterone receptor (PR), and human epidermal growth factor receptor 2 (HER-2) [12,13]. Furthermore, advances in gene expression profiling have led to the molecular classification of breast cancer (e.g., luminal A, luminal B, HER-2-enriched, and triple-negative), which plays a pivotal role in guiding targeted and individualized therapies [11,14]. In recent years, the integration of multiparametric MRI—combining DCE-MRI, diffusion-weighted imaging (DWI), and T2-weighted imaging—has significantly advanced the noninvasive prediction of these molecular subtypes [15]. Current evidence highlights distinct imaging phenotypes among subtypes; for instance, HER-2-overexpressing tumors are significantly more likely to manifest as non-mass enhancement (NME), often demonstrating segmental distribution or clumped enhancement, whereas triple-negative and luminal breast cancers predominantly present as distinct mass lesions [15,16].

In contemporary breast MRI interpretation, the American College of Radiology (ACR) Breast Imaging Reporting and Data System (BI-RADS) lexicon provides a standardized framework. While mass lesions are relatively straightforward to characterize, NME presents a unique diagnostic challenge. NME exhibits variable morphological and kinetic features that frequently overlap between benign conditions (e.g., fibrocystic changes) and malignant etiologies (e.g., ductal carcinoma in situ or invasive carcinoma). Although the correlation between BI-RADS NME descriptors and histopathology has been widely explored, imaging features are rarely integrated with molecular subtypes and cellular proliferation indices. Furthermore, recent research has emphasized the critical role of the Ki-67 proliferation index as a marker of tumor aggressiveness and heterogeneity [17]. While conventional visual assessment of BI-RADS descriptors provides a fundamental diagnostic framework, contemporary research is increasingly shifting toward multiparametric and quantitative image analyses to characterize complex tumor heterogeneity [18,19]. Integrating these advanced imaging features to accurately predict Ki-67 expression levels and specific molecular subtypes before surgery remains an area of active investigation [18,20].

Therefore, this study aims to retrospectively evaluate the morphological distribution patterns, internal enhancement characteristics, and kinetic features of NME on breast MRI according to the BI-RADS lexicon (5th edition, 2013) and to correlate these findings with definitive histopathological diagnoses. Specifically, we aim to investigate the potential predictive value of NME imaging features for breast cancer molecular subtypes and the Ki-67 proliferation index in malignant lesions.

Although emerging artificial intelligence and radiomics models have gained popularity for predicting Ki-67 expression and molecular subtypes, these methods often require specialized software and extensive computational resources, limiting their adoption in routine clinical practice. This study addresses a critical knowledge gap by demonstrating that routine, standardized BI-RADS morphological descriptors can serve as noninvasive, accessible surrogate markers of tumor biological aggressiveness, facilitating rapid risk stratification in clinical workflows without the need for additional complex processing.

Materials and Methods

Study Design and Patient Population

This retrospective cohort study was conducted at the Department of Radiology, Faculty of Medicine, of our tertiary academic center. The study protocol was approved by the institutional review board, and the requirement for informed consent was waived due to the retrospective nature of the study. We evaluated dynamic contrast-enhanced (DCE) breast MRI examinations performed between January 2013 and November 2015. Patients were included if they presented with non-mass enhancement (NME) on breast MRI and had definitive histopathological diagnoses available in the institutional database. Patients with incomplete imaging data or concomitant suspicious mass lesions were excluded from the analysis. A total of 61 patients (age range: 13–75 years; mean age: 48 years) with 62 isolated NME lesions were included in the final study cohort.

Ethical Considerations

The study was conducted in accordance with the principles of the Declaration of Helsinki. The study protocol was reviewed and approved by the Ege University Medical Research Ethics Committee (approval date: December 28, 2015; decision no. 15-12.1/47). The requirement for informed consent was waived by the ethics committee due to the retrospective nature of the study.

Imaging Protocol

Breast MRI examinations were performed using 1.5-T (Siemens Symphony Vision, Siemens Healthineers, Erlangen, Germany) and 3-T (Siemens Verio, Siemens Healthineers, Erlangen, Germany) scanners equipped with dedicated bilateral breast coils. The standard imaging protocol included axial T1-weighted and T2-weighted fat-suppressed images, followed by DCE sequences acquired before and at multiple time points after the intravenous administration of a gadolinium-based contrast agent (0.1 mmol/kg). Key sequence parameters for T1-weighted sequences included a repetition time (TR) of 5.5 ms, an echo time (TE) of 1.78 ms, a slice thickness of 1 mm, a field of view (FOV) of 280 mm, and a matrix size of 320×320. The DCE series were acquired with a temporal

resolution of approximately 60 seconds per phase. Subtraction images were generated to highlight areas of enhancement.

Image Interpretation

Two board-certified breast radiologists (with 15 and 5 years of experience in breast imaging, respectively) independently reviewed all MRI examinations [21]. Both readers were blinded to the patients' clinical data, original radiological reports, and final histopathological diagnoses. NME features were characterized according to the American College of Radiology (ACR) BI-RADS lexicon (5th edition, 2013). The evaluation included distribution patterns, internal enhancement characteristics, background parenchymal enhancement (BPE), and associated findings. Time-intensity curves (TICs) were extracted from the most avidly enhancing portion of the NME and classified into three types based on the delayed phase: persistent (type I), plateau (type II), or washout (type III). In cases of disagreement regarding BI-RADS NME descriptors or kinetic curve assessment, consensus was reached through discussion.

Histopathological and Molecular Correlation

Histopathological results obtained through image-guided biopsy or surgical excision served as the reference standard. The expression levels of ER, PR, HER-2, and the Ki-67 proliferation index were determined using immunohistochemistry (IHC). ER and PR positivity were defined as nuclear staining in ≥1% of tumor cells. HER-2 status was considered positive if the IHC score was 3+, whereas tumors with an equivocal score of 2+ underwent fluorescence in situ hybridization (FISH) to confirm gene amplification [22].

Ki-67 expression was evaluated using two distinct categorization approaches based on the analytical objective. First, for molecular subtyping, a 14% cutoff was adopted based on the 2011 St. Gallen International Expert Consensus criteria (Goldhirsch et al., 2011) [23] to help distinguish luminal A (Ki-67<14%) from luminal B (Ki-67≥14%) subtypes, consistent with the histopathological classification approach used at our institution during the study period. Second, to evaluate the relationship between NME spatial distribution patterns and tumor proliferation, Ki-67 values were grouped into three categories (<10%, 10–30%, and >30%). The <10% category was used to identify tumors with low proliferative activity [24].

Breast cancer molecular subtypes were classified as luminal A, luminal B, HER-2-enriched, and triple-negative based on these profiles.

Statistical Analysis

Data were analyzed using IBM SPSS Statistics version 21.0 (IBM Corp., Armonk, NY, USA). Descriptive statistics were used to summarize patient demographics and imaging findings. Categorical variables, including NME distribution patterns, internal enhancement features, BPE, molecular subtypes, and Ki-67 proliferation categories, were compared using Pearson's chi-square test or Fisher's exact test when expected cell counts were less than 5. Exact p-values and effect size estimates (Cramér's V or odds ratios with 95% confidence intervals [CIs]) were reported where appropriate.

The relationships between BI-RADS descriptors (distribution pattern, internal enhancement, and BPE) and histopathological results (benign vs. malignant status, molecular subtypes, and Ki-67 expression) were evaluated using Pearson's chi-square test and Fisher's exact test.

Ki-67 expression was evaluated as a categorical variable. In accordance with the St. Gallen International Expert Consensus criteria, a 14% threshold was adopted to differentiate luminal A from luminal B molecular subtypes. Additionally, to analyze spatial heterogeneity across NME distribution patterns, Ki-67 values were categorized into clinically relevant proliferation tiers (<10%, 10–30%, and >30%).

Given the limited sample size (61 patients, 62 lesions, and 41 malignant cases) and the risk of model overfitting, multivariable logistic regression was not performed. This decision was based on the events-per-variable (EPV) consideration of approximately 10–15 events per predictor variable. Instead, univariable comparisons were performed. Interobserver agreement for BI-RADS descriptors was assessed using Cohen's kappa (κ) statistic [23]. A p-value <0.05 was considered statistically significant [15].

Results

Patient Demographics and Histopathological Findings

The baseline clinicopathological characteristics and imaging findings of the final study cohort (n=61) are summarized in **Table 1**. The final study cohort comprised 61 female patients with 62 isolated non-mass enhancement (NME) lesions. The mean patient age was 48.19±11.31 years (range: 13–75 years). Based on histopathological evaluation, 41 lesions (66.1%) were malignant, and 21 lesions (33.9%) were benign. Among the malignant lesions, invasive ductal carcinoma (IDC) was the most common histological subtype (n=27, 43.5%), followed by ductal carcinoma in situ (DCIS) (n=6, 9.7%) and invasive lobular carcinoma (ILC) (n=5, 8.1%). According to the immunohistochemical classification of the 41 malignant lesions, 17 (41.4%) were luminal A, 14 (34.1%) were luminal B, 7 (17.0%) were HER-2-enriched, and 3 (7.3%) were triple-negative. The patient selection process is detailed in Figure 1.

Table 1. Baseline demographic characteristics, background parenchymal enhancement, and additional MRI findings of benign and malignant non-mass enhancement lesions

Variable	Benign (n=21)	Malign (n=41)	p
Age (Years)			0.129
<48	7 (33.3)	22 (53.7)	
≥48	14 (66.7)	19 (46.3)	
Bpe Degree			**0.020**
Minimal	12 (57.1)	19 (46.3)	
Mild	4 (19.0)	4 (9.8)	
Moderate	5 (23.8)	6 (14.6)	
Marked	0 (0.0)	12 (29.3)	
BPE Symmetry			**0.038**
Symmetric	19 (90.5%)	26 (63.4%)	
Asymmetric	2 (9.5%)	15 (88.2%)	
Additional Findings*			**0.024**
Absent	19 (90.5)	26 (63.4)	
Present	2 (9.5)	15 (36.6)	

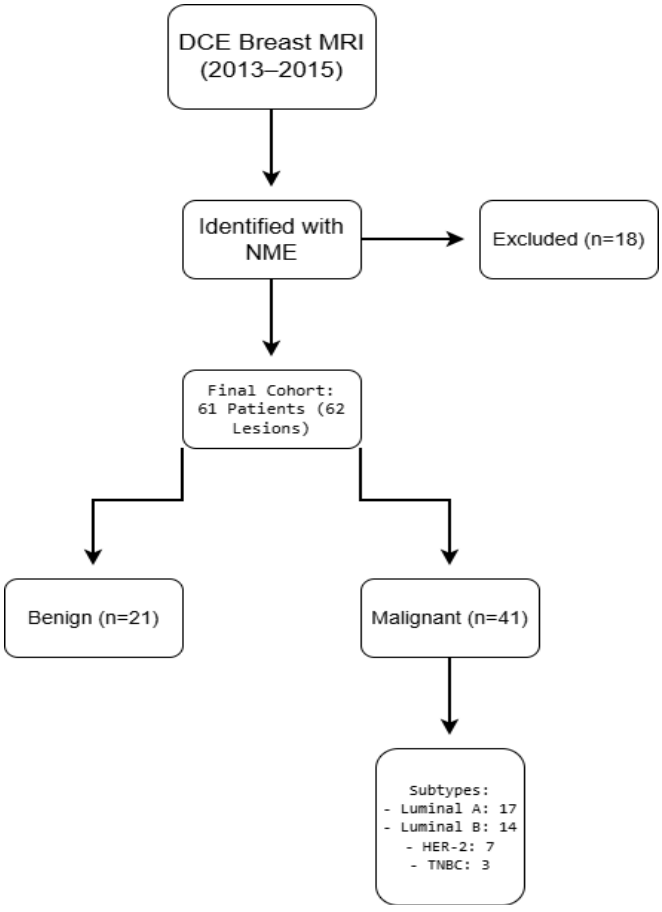

Figure 1. Flowchart of patient selection and lesion classification based on final histopathological and molecular subtype analysis

Morphological MRI Features and Malignancy Prediction

The distribution pattern of NME demonstrated a highly significant correlation with malignancy (p=0.002). Focal distribution was predominantly associated with benign pathology (68.8% benign), whereas linear and segmental distributions were strongly predictive of malignancy (73.7% malignant). Furthermore, regional, multiregional, and diffuse distribution patterns exhibited the highest risk of malignancy (81.5% malignant) (Table 2). Representative MRI cases demonstrating benign focal NME and malignant segmental NME with clumped enhancement are illustrated in Figures 2 and 3, respectively.

Regarding internal enhancement characteristics, although heterogeneous internal enhancement was frequently observed in both groups, it did not provide statistically significant discrimination between benign and malignant etiologies (52.4% vs. 48.8%, respectively; p=0.284). Conversely, clustered ring and clumped enhancement patterns were significantly associated with malignancy, with specificities of 95.2% and 90.5%, respectively (p<0.001).

The degree and symmetry of background parenchymal enhancement (BPE) served as significant predictors of malignancy (p=0.020). Notably, extreme BPE presentations carried the highest risk; all lesions occurring in the setting of marked BPE were confirmed as malignant, and asymmetric BPE was associated with an 88% malignancy rate. The presence of additional MRI findings (e.g., nipple retraction, skin thickening, and structural distortion) was significantly correlated with a higher likelihood of malignancy (88.2% vs. 57.8% in patients without additional findings; p=0.024). Kinetic curve assessments did not reveal a statistically significant difference between the benign and malignant groups (p=0.392).

Table 2. Diagnostic performance of BI-RADS NME morphological descriptors

Feature	Benign (n=21)	Malign (n=41)	p
Distribution Pattern			**0.002**
Focal	11 (52.4)	5 (12.2)	
Linear	3 (14.3)	2 (4.9)	
Segmental	2 (9.5)	12 (29.3)	
Regional	4 (19.0)	5 (12.2)	
Multiregional	1 (4.8)	13 (31.7)	
Diffuse	0 (0.0)	4 (9.8)	
Internal Enhancement			0.284
Homogeneous	7 (33.3)	5 (12.2)	
Heterogeneous	11 (52.4)	20 (48.8)	
Clumped	2 (9.5)	7 (17.1)	
Clustered Ring	1 (4.8)	9 (22.0)	

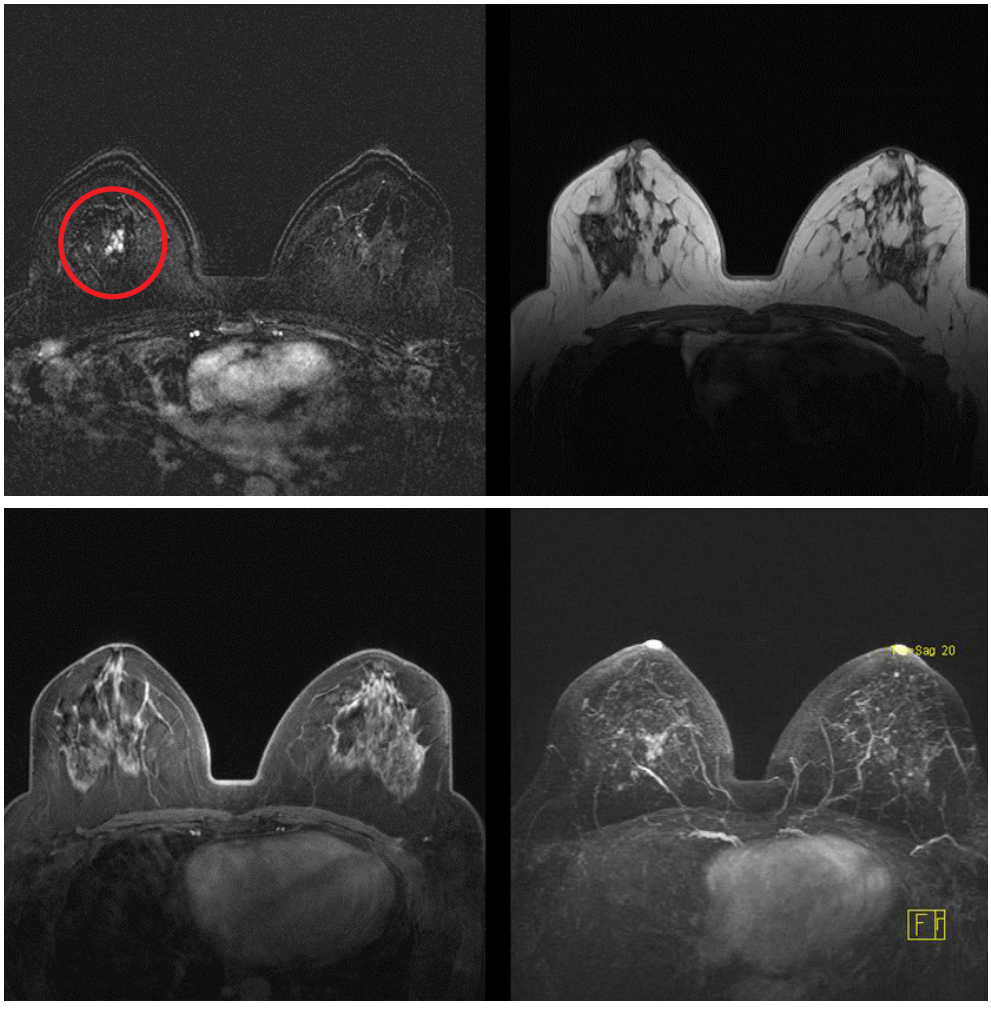

Figure 2. Axial dynamic contrast-enhanced breast MRI of a 47-year-old female patient demonstrating focal non-mass enhancement (NME) in the right breast. The lesion exhibits a heterogeneous internal enhancement pattern. Definitive histopathology confirmed benign fibrocystic changes, illustrating the biologically indolent nature and limited spatial heterogeneity characteristically associated with focal distribution patterns.

Interobserver agreement between the two breast radiologists was evaluated for all primary BI-RADS NME descriptors. Overall, interobserver agreement ranged from substantial to almost perfect across features. Substantial agreement was achieved for spatial distribution patterns (κ=0.76, 95% CI: 0.63–0.89) and internal enhancement characteristics (κ=0.69, 95% CI: 0.54–0.84). High agreement was also demonstrated for BPE degree assessment (κ=0.72, 95% CI: 0.57–0.87), BPE symmetry (κ=0.81, 95% CI: 0.68–0.94), and kinetic curve patterns (κ=0.74, 95% CI: 0.59–0.89). Detailed interobserver agreement statistics are summarized in Table 3.

Correlation with Molecular Subtypes and Ki-67 Proliferation Index

Intrinsic molecular subtyping (luminal A vs. luminal B), based on the 2011 St. Gallen Ki-67 cutoff of 14%, was not significantly associated with NME morphological descriptors (p>0.05). However, when Ki-67 expression was evaluated using proliferation categories (<10%, 10–30%, and >30%), a statistically significant association was observed between NME distribution patterns and Ki-67 expression (Pearson's chi-square test, p=0.037). Specifically, all five focal malignant NME lesions (100%, 5/5) had a low Ki-67 index (<10%). When focal NME was compared with nonfocal distribution patterns (linear, segmental, regional, multiregional, and diffuse), focal distribution was significantly associated with low Ki-67 expression (<10% vs. ≥10%; Fisher's exact test, p=0.015). In contrast, extensive enhancement patterns (segmental, diffuse, and multiregional) were more frequently associated with elevated Ki-67 expression (≥10%).

This observation aligns with contemporary radiomic concepts, suggesting that rapid cellular proliferation and subsequent microenvironmental hypoxia manifest as spatially heterogeneous and morphologically diffuse enhancement patterns on MRI [25,26].

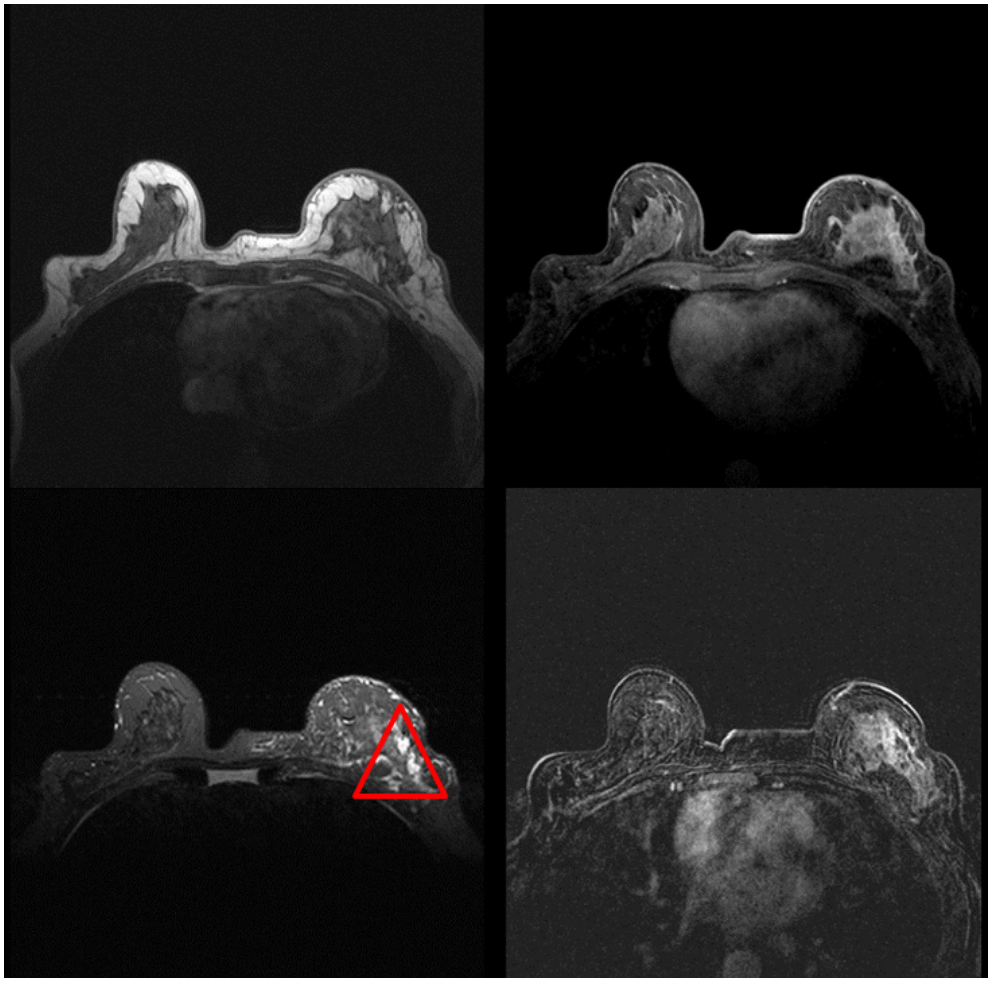

Figure 3. Axial dynamic contrast-enhanced breast MRI of a 53-year-old female patient demonstrating malignant non-mass enhancement (NME) in the left breast. The lesion shows a distinct segmental distribution with a clustered ring internal enhancement pattern. Definite histopathological analysis confirmed invasive ductal carcinoma (Luminal B subtype) with an elevated Ki-67 index, reflecting aggressive ductal spread and active angiogenesis.

Table 3. Inter-observer agreement (Cohen's Kappa) for BI-RADS NME descriptors between two breast radiologists

BI-RADS Descriptor	Observed Agreement (%)	Cohen's Kappa (κ)	95% Confidence Interval (CI)	Agreement Level
Spatial Distribution Pattern	83.9%	**0.76**	0.63 – 0.89	Substantial
Internal Enhancement Pattern	79.0%	**0.69**	0.54 – 0.84	Substantial
BPE Degree	82.3%	**0.72**	0.57 – 0.87	Substantial
BPE Symmetry	88.7%	**0.81**	0.68 – 0.94	Almost Perfect
Kinetic Curve Type	83.9%	**0.74**	0.59 – 0.89	Substantial

BPE: Background Parenchymal Enhancement. Landis and Koch criteria were applied for agreement interpretation (0.61–0.80: Substantial; 0.81–1.00: Almost Perfect).

Discussion

Principal Findings

In this retrospective cohort study, we comprehensively evaluated the morphological distribution, internal enhancement characteristics, and kinetic features of non-mass enhancement (NME) on breast MRI, correlating these findings with definitive histopathology and molecular subtypes. Our findings suggest that the spatial distribution pattern of NME and the degree of background parenchymal enhancement

Table 4. Diagnostic performance metrics of NME features

Feature	Sensitivity (%)	Specificity (%)	PPV (%)	NPV (%)
Segmental Distribution	29.3	90.5	85.7	39.6
Multiregional Distribution	31.7	95.2	92.9	41.7
Diffuse Distribution	9.8	100.0	100.0	36.2
Clustered Ring Enhancement	22.0	95.2	90.0	38.5
Clumped Enhancement	17.1	90.5	77.8	35.8

(BPE) are imaging features significantly associated with malignancy.

Furthermore, we report a striking and novel correlation between the focal distribution pattern of malignant NME and a significantly low Ki-67 proliferation index (<10%), highlighting the potential of MRI to noninvasively reflect spatial tumor heterogeneity and intrinsic biological aggressiveness.

Demographics and Population Analysis

The demographic profile and malignancy distribution of our study cohort (61 patients, 62 lesions; mean age: 48.19 years) demonstrate intriguing similarities and differences when compared with the pioneering NME literature. Our sample size is highly comparable to those of other established single-center retrospective cohorts evaluating isolated NME, such as the series reported by Cho et al. [25] (n=88), Ballesio et al. [26] (n=94), Newell et al. [27] (n=116), Dratwa et al. [28] (n=119), and Thomassin-Naggara et al. [29] (n=131).

Notably, the malignancy rate observed in our study (66.1%) was higher than those reported by Dratwa et al. [28] (18.9%), Newell et al. [27] (39.0%), and Thomassin-Naggara et al. [29] (42.7%), yet remained lower than the malignancy rate documented by Cho et al. [25] (83.0%). This distinct distribution was largely driven by our strict inclusion criteria, which explicitly excluded cases with accompanying mass lesions (n=18) and focused exclusively on histopathologically verified isolated NME lesions managed at a tertiary academic referral center. Such a clinical setting inherently results in a preselected patient group with a higher pretest probability of malignancy, emphasizing that isolated NME encountered in tertiary care databases carries an elevated clinical risk and necessitates careful optimization of biopsy criteria to prevent false-negative assessments.

NME Distribution Patterns and Malignancy Prediction

In the present study, the spatial distribution pattern of NME emerged as a robust and highly significant imaging biomarker for malignancy (p=0.002). Consistent with contemporary radiologic-pathologic paradigms, our analysis revealed that extensive enhancement distributions—specifically segmental, multiregional, and diffuse patterns—yielded exceptionally high malignancy rates, ranging from 81.5% to 100%. These results build upon earlier foundational studies; for instance, Thomassin-Naggara et al. [29] and Dratwa et al. previously reported that malignant NME predominantly manifests in segmental or regional distributions, reflecting the ductal anatomy of the breast. Similarly, Cho et al. [25] highlighted a 93.3% specificity for segmental distribution in predicting malignancy. Recent investigations corroborate and extend these earlier findings, underscoring that segmental distribution is a hallmark of malignant ductal spread and extensive tumor angiogenesis, frequently yielding positive predictive values (PPVs) exceeding 80% [30,31]. This macroscopic imaging presentation directly reflects the biological tendency of high-grade in situ and invasive carcinomas (such as DCIS and IDC) to aggressively infiltrate along the ductal networks.

Conversely, focal NME distribution in our cohort was predominantly associated with benign etiologies (68.8%). This observation parallels recent evidence demonstrating that localized focal enhancement typically reflects benign proliferative changes or fibrocystic disease with limited spatial heterogeneity rather than malignant progression [32]. Ultimately, our findings validate the use of macroscopic NME distribution patterns as a critical noninvasive risk stratification tool. Integrating these spatial features into routine clinical decision-making underscores the clinical importance of prompt tissue sampling for segmental or diffuse lesions while offering a potential basis for safely minimizing unnecessary interventions for purely focal enhancement.

The Ki-67 Milestone and Spatial Tumor Heterogeneity

A key finding of our study is the strong association between focal NME distribution and a low Ki-67 proliferation index (<10%), in stark contrast to the higher Ki-67 indices (>10–30%) observed in diffuse, segmental, and multiregional patterns. This phenomenon can be explained through the lens of modern tumor biology, specifically the interplay among rapid cellular proliferation, intratumoral hypoxia, and neoangiogenesis. Contemporary research indicates that a high Ki-67 index reflects aggressive cellular proliferation that rapidly outstrips the

local vascular supply, generating a microenvironment highly prone to ischemia and hypoxia. This hypoxic state acts as a catalyst for chaotic angiogenesis and increased vascular permeability, which manifest macroscopically on MRI as extensive, infiltrative NME patterns (e.g., segmental or diffuse) [33] (Fig. 3). Consequently, the pronounced spatial tumor heterogeneity inherent in highly proliferative tumors is reflected in these extensive distributions, whereas focal NME lesions represent biologically indolent, localized lesions with balanced perfusion and limited spatial heterogeneity [33] (Fig. 2).

The Clinical Significance of BPE and Kinetic Ineffectiveness

Furthermore, our analysis revealed that while marked and asymmetric background parenchymal enhancement (BPE) was significantly associated with malignancy (88–100% malignancy rate, p=0.020), traditional kinetic curve assessments (types I, II, and III) failed to distinguish between benign and malignant NME lesions (p=0.392). Although type III (washout) kinetic curves are highly specific for malignant mass lesions—owing to their dense cellularity and uniform aberrant neovascularization—their diagnostic utility is significantly compromised in NME lesions. Recent literature attributes this limitation to the inherent infiltrative growth pattern of NME, which characteristically features interspersed normal fibroglandular tissue and fat within the enhancing abnormality [29,34]. During the extraction of time-intensity curves, the inadvertent inclusion of intervening normal breast parenchyma within the region of interest (ROI) leads to substantial partial volume effects [29]. This signal averaging dampens the classic rapid wash-in and washout dynamics of malignant angiogenesis, causing aggressive NME lesions to frequently exhibit nondiagnostic persistent or plateau curves. In contrast, marked asymmetry in BPE likely reflects global hormonal or angiogenic stimulation of the entire breast tissue harboring the malignancy, thereby remaining a reliable macroscopic indicator of breast cancer presence.

Our study has certain limitations, most notably its retrospective, single-center design and the relatively small cohort of 61 patients. However, rather than representing a definitive constraint, this focused dataset serves as an essential foundation for further research. To ensure high diagnostic reliability and minimize subjective interpretation, we strengthened our methodology by incorporating a rigorous interobserver agreement analysis using Cohen's kappa statistics. Ultimately, our findings provide a preliminary pathophysiological foundation that paves the way for future large-scale, prospective multicenter trials. Furthermore, integrating these detailed macroscopic MRI features into emerging artificial intelligence and deep learning frameworks will be critical for overcoming human variability and unlocking the full potential of automated, high-throughput tumor phenotyping [35].

In conclusion, our findings suggest that NME spatial distribution patterns may provide useful imaging information for malignancy risk stratification. In particular, the observed association between focal NME and low Ki-67 expression may reflect differences in tumor proliferation. However, these imaging features should not be considered definitive indicators of biological aggressiveness or independent predictors of malignancy. Given the retrospective, single-center design and relatively small sample size, our results should be interpreted as exploratory. Larger prospective, multicenter studies are needed to validate these associations and assess their potential role in clinical decision-making.

Ethics

Ethics Committee Approval: The study protocol was approved by the Ege University Medical Research Ethics Committee (Approval Date: 28.12.2015 , Decision No: 15-12.1/47).

Informed Consent: The requirement for informed consent was waived by the ethics committee due to the retrospective nature of the study.

Conflict of Interest: The authors declare that the research was conducted without any commercial or financial relationships that could be construed as a potential conflict of interest.

Financial Disclosure: The authors received no financial support for the research, authorship, and/or publication of this article.

Use of AI for Writing Assistance: None declared.

Data Availability Statement: The data that support the findings of this study are available from the corresponding author upon reasonable request. Image data were extracted and processed from the clinical PACS (Sectra AB, Linköping, Sweden) at the Ege University Medical School using Digital Imaging and Communications in Medicine (DICOM) query/retrieve software. The PACS system is closed to external users. All clinical data, including laboratory and clinical follow-up, were obtained from the Ege University Hospital Electronic Patient File Repository. The Electronic Patient File Repository is closed to external users. Data are provided in a spreadsheet format (Microsoft Excel). The spreadsheet is secured and deposited by the corresponding author.

Authorship Contributions: Concept: M.K., U.D.P.; Design: U.D.P, Ö.S.O.; Resource: M.K., U.D.P., Ö.S.O.; Materials: M.K., U.D.P., Ö.S.O., A.O.A., I.B.; Data collection and/or processing: Ö.S.O., A.O.A., I.B.; Analysis and/or interpretation: M.K., U.D.P., I.B.; Literature review: M.K., U.D.P., Ö.S.O., A.O.A., I.B.; Writing: U.D.P., Critical review: M.K., U.D.P., Ö.S.O., A.O.A., I.B.

Peer-review: Externally peer-reviewed.

References

1. Hortobagyi GN, de la Garza Salazar J, Pritchard K, Amadori D, Haidinger R, Hudis CA, et al. The global breast cancer burden: variations in epidemiology and survival. Clin Breast Cancer 2005;6:391-401.
2. Kopans DB. The positive predictive value of mammography. AJR Am

J Roentgenol 1992;158:521-6.

3. Carney PA, Miglioretti DL, Yankaskas BC, Kerlikowske K, Rosenberg R, Rutter CMet al. Individual and combined effects of age, breast density, and hormone replacement therapy use on the accuracy of screening mammography. Ann Intern Med 2003;138:168-75. https://doi.org/10.7326/0003-4819-138-3-200302040-00008
4. Szabó BK, Aspelin P, Kristoffersen Wiberg M, Tot T, Boné B. Invasive breast cancer: correlation of dynamic MR features with prognostic factors. Eur Radiol 2003;13:2425-35.
5. Kerlikowske K, Grady D, Barclay J, Sickles EA, Ernster V. Likelihood ratios for modern screening mammography. Risk of breast cancer based on age and mammographic interpretation. JAMA 1996;276:39-43.
6. Leung JW. Screening mammography reduces morbidity of breast cancer treatment. AJR Am J Roentgenol 2005;184:1508-9.
7. Kolb TM, Lichy J, Newhouse JH. Comparison of the performance of screening mammography, physical examination, and breast US and evaluation of factors that influence them: an analysis of 27,825 patient evaluations. Radiology 2002;225:165-75.
8. Segel MC, Paulus DD, Hortobagyi GN. Advanced primary breast cancer: assessment at mammography of response to induction chemotherapy. Radiology 1988;169:49-54.
9. Boulogianni G, Chryssogonidis I, Drevelegas A. Diffusion weighted MRI and spectroscopy in invasive carcinoma of the breast at 3Tesla. Correlation with dynamic contrast enhancement and pathologic findings. Hippokratia 2016;20:192-7.
10. Çelebiler Çavuşoğlu A, Saydam S, Canda T, Sakızlı M. Meme tümör sınıflamasında yenilik çabaları. Meme Sağlığı Dergisi 2009;5:187-90. [in Turkish]
11. Contesso G, Mouriesse H, Friedman S, Genin J, Sarrazin D, Rouesse J. The importance of histologic grade in long-term prognosis of breast cancer: a study of 1,010 patients, uniformly treated at the Institut Gustave-Roussy. J Clin Oncol 1987;5:1378-86.
12. Stewart JF, Rubens RD, Millis RR, King RJ, Hayward JL. Steroid receptors and prognosis in operable (stage I and II) breast cancer. Eur J Cancer Clin Oncol 1983;19:1381-7.
13. Donegan WL. Tumor-related prognostic factors for breast cancer. CA Cancer J Clin 1997;47:28-51.
14. Eroğlu A, Çiçek E. Meme Kanserinde moleküler alt tiplere göre cerrahi tedavi yaklaşımları. Yeni Tıp Dergisi 2014;31:83-7. [in Turkish]
15. Li J, Huo G, Lei X, Li G, Yu M, Nie Z, et al. Correlation analysis of multiparametric magnetic resonance imaging features and molecular subtypes of breast cancer. J Clin Imaging Sci 2025;15:37.
16. El-Rawy AS, Gaballa A, Shafik A, Ramadan M, Yones H. Magnetic resonance imaging correlation with molecular and epigenetic markers in assessment of breast cancer. Egypt J Radiol Nucl Med 2022;53:211.
17. Liu J, Wang X, Hu M, Zheng Y, Zhu L, Wang W, Hu J, et al. Development of an ultrasound-based radiomics nomogram to preoperatively predict Ki-67 expression level in patients with breast cancer. Front Oncol 2022;12:963925.
18. Wang Q, Zheng N, Yu Q, Shao S. Multimodal imaging and advanced quantitative techniques for HER-2 status prediction in breast cancer. Discov Oncol 2025;16:1820.
19. Pinker K, Chin J, Melsaether AN, Morris EA, Moy L. Precision medicine and radiogenomics in breast cancer: new approaches toward diagnosis and treatment. Radiology 2018;287:732–47.
20. Li JW, Sheng DL, Chen JG, You C, Liu S, Xu HX, et al. Artificial intelligence in breast imaging: potentials and challenges. Phys Med Biol 2023;68.
21. Lunkiewicz M, Forte S, Freiwald B, Singer G, Leo C, Kubik-Huch RA. Interobserver variability and likelihood of malignancy for fifth edition BI-RADS MRI descriptors in non-mass breast lesions. Eur Radiol 2020;30:77–86.
22. Shen Y, Zhang X, Zheng J, Wang S, Ding J, Sun S, et al. Distinguishing low expression levels of human epidermal growth factor receptor 2 in breast cancer: Insights from qualitative and quantitative magnetic resonance ımaging analysis. Tomography 2025;11:31.
23. Goldhirsch A, Wood WC, Coates AS, Gelber RD, Thürlimann B, Senn HJ, et al. Strategies for subtypes--dealing with the diversity of breast cancer: highlights of the St. Gallen International Expert Consensus on the Primary Therapy of Early Breast Cancer 2011. Ann Oncol Off J Eur Soc Med Oncol 2011;22:1736–47..
24. Liu X, Liu Y, Ma T, Zhang S, Liu L, Wang S, et al. Clinicopathological and imaging factors of surgical margin status and prognosis in breast-conserving therapy. Sci Rep 2026;16:10450.
25. Cho YH, Cho KR, Park EK, Seo BK, Woo OH, Cho SB. Significance of additional non-mass enhancement in patients with breast cancer on preoperative 3t dynamic contrast enhanced MRI of the breast. Iran J Radiol 2016;13:e30909.
26. Ballesio L, Di Pastena F, Gigli S, D'ambrosio I, Aceti A, Pontico M, et al. Non mass-like enhancement categories detected by breast MRI and histological findings. Eur Rev Med Pharmacol Sci 2014;18:910-7.
27. Newell D, Nie K, Chen JH, Hsu CC, Yu HJ, Nalcioglu O. Selection of diagnostic features on breast MRI to differentiate between malignant and benign lesions using computer-aided diagnosis: differences in lesions presenting as mass and non-mass-like enhancement. Eur Radiol 2010;20:771–81.
28. Dratwa C, Jalaguier-Coudray A, Thomassin-Piana J, Gonin J, Chopier J, Antoine M. Breast MR biopsy: Pathological and radiological correlation. Eur Radiol 2016;26:2510–9.
29. Thomassin-Naggara I, Trop I, Chopier J, David J, Darai E, Uzan S, et al. Nonmasslike enhancement at breast MR imaging: the added value of mammography and US for lesion categorization. Radiology 2011;261:69–79.
30. Elboghdady AA, Shawky SA, Mohsen M, Zaky MM. Can early post-operative MRI describe a predictor model for the likelihood of early breast cancer recurrence after conservative surgery? Egypt J Radiol Nucl Med 2024;55:103.
31. Kareem TF, Kamal AM, Nakash MA. Dynamic curve type serves as an effective tool for the diagnosis of benign or malignant non-mass enhancements on breast MRI. Oncol Lett 2026;31:212.
32. Pötsch N, Dietzel M, Kapetas P, Clauser P, Pinker K, Ellmann S. An A.I. classifier derived from 4D radiomics of dynamic contrast-enhanced breast MRI data: potential to avoid unnecessary breast biopsies. Eur Radiol 2021;31:5866–76.
33. Goto Y, Ochi T, Sakaguchi Y, Yoshida T, Fujitani S, Maeda K. Usefulness of computed tomography angiography "spot sign" in the endoscopically assisted evacuation of acute subdural hematoma in the elderly. Interdiscip Neurosurg Adv Tech Case Manag 2021;24.
34. Ziada K, Aggarwal R, Siu M, Jallad N, Gatt R, Al-Attar M. Comparison of preoperative breast cancer disease extent on contrast-enhanced mammography (CEM) versus magnetic resonance imaging (MRI. Clin Radiol 2026;98.